Carbon Contamination of Extreme Ultraviolet (EUV) Masks and its Effect on Imaging

Yu-Jen Fan[1], Leonid Yankulin[1], Alin Antohe[1], Rashi Garg[1], Petros Thomas[1], Chimaobi Mbanaso[1], Andrea Wüest[2], Frank Goodwin[2], Sungmin Huh[2], Patrick Naulleau[3], Kenneth Goldberg[3], Iacopo Mochi[3], Gregory Denbeaux[1]

1. College of Nanoscale Science and Engineering, University at Albany SUNY
2. SEMATECH, Albany, NY
3. CXRO, Lawrence Berkeley National Laboratory, Berkeley CA

ABSTRACT

Carbon contamination of extreme ultraviolet (EUV) masks and its effect on imaging is a significant issue due to lowered throughput and potential effects on imaging performance. In this work, a series of carbon contamination experiments were performed on a patterned EUV mask. Contaminated features were then inspected with a reticle scanning electron microscope (SEM) and printed with the SEMATECH Berkeley Microfield-Exposure tool (MET) [1]. In addition, the mask was analyzed using the SEMATECH Berkeley Actinic-Inspection tool (AIT) [2] to determine the effect of carbon contamination on the absorbing features and printing performance.

To understand the contamination topography, simulations were performed based on calculated aerial images and resist parameters. With the knowledge of the topography, simulations were then used to predict the effect of other thicknesses of the contamination layer, as well as the imaging performance on printed features.

Keywords: EUV mask, carbon contamination, Shadowing effect, CD compensation

1. INTRODUCTION

EUV lithography (EUVL) is one of the leading candidates for next generation lithography; however, there are remaining challenges before EUVL is ready for high volume manufacturing (HVM) introduction. Carbon contamination is one of the critical issues, and occurs in ultra high vacuum (UHV) EUV exposure tools due to the presence of residual carbon containing molecules.

The impact of carbon contamination on patterned EUV masks is not well understood. Apart from reflectivity, and hence throughput loss, additional effects on imaging performance in terms of critical dimension (CD) error, dose shift can occur. In order to investigate the influence of carbon contamination, we built the EUV Microscope for Mask Imaging and Contamination Study (MiMICS) [3]. This tool is equipped with a Xe plasma EUV source, and allows us to contaminate the EUV masks intentionally and in a control fashion by injecting carbon containing molecules into the vacuum chamber.

After contamination, the mask was investigated by printing features and aerial image analysis. The images were printed at the SEMATECH Berkeley MET, and the exposed wafers were analyzed using a SEM to measure the CD at the best focus as a function of dose and exposure time. We also used the SEMATECH Berkeley AIT to record the intensity profile of aerial images from selected regions of the EUV mask. The process window and contrast curves were also measured.

Simulations were applied to understand the carbon contamination topography on EUV masks. Two extreme assumptions of topography were developed based on experimental data of printed features. Aerial images and resist parameters were then calculated using the Panoramic software [4]. With the knowledge of the topography, simulations were used to predict the limitations of allowed carbon thickness with optical correction.

Alternative Lithographic Technologies, edited by Frank M. Schellenberg, Bruno M. La Fontaine
Proc. of SPIE Vol. 7271, 72713U · © 2009 SPIE · CCC code: 0277-786X/09/$18 · doi: 10.1117/12.814196

2. EXPERIMENT

Intentional contamination was performed using the EUV MiMICS at the College of Nanoscale Science and Engineering (CNSE), University at Albany. This tool was specially designed to evaluate the impact of carbon contamination on patterned masks, as well as the sources of contamination for EUV masks.

The layout of the MiMICS tool is shown in **Figure 1.** This tool was developed in 2006, and equipped with Xe plasma EUV source, producing 13.5-nm EUV radiation, as well as a EUV sensitive CCD camera. The illuminating beam passes through a Si/Zr filter and reflects off a multilayer mirror, with 6° off-axis angle-of-incidence (AOI) onto a mask.

In order to produce the contamination on the EUV mask at a faster rate, we injected carbon containing molecules into the chamber using a needle valve. A 3 by 5 mm aperture was also used to only contaminate desired features within a selected area, and a picture of such a contaminated area on a EUV mask is shown in **Figure 2**.

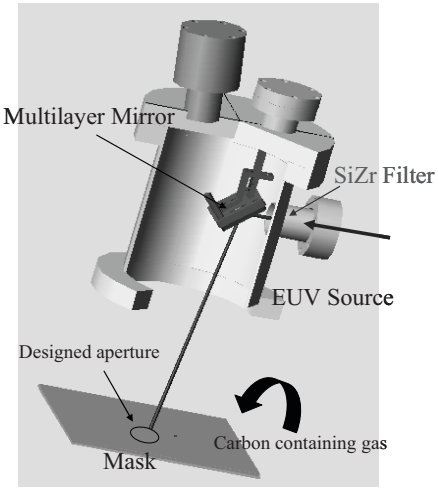

Fig. 1. Layout of the EUV MiMICS at Albany. Carbon containing molecules were injected near the mask surface to produce a faster contamination rate.

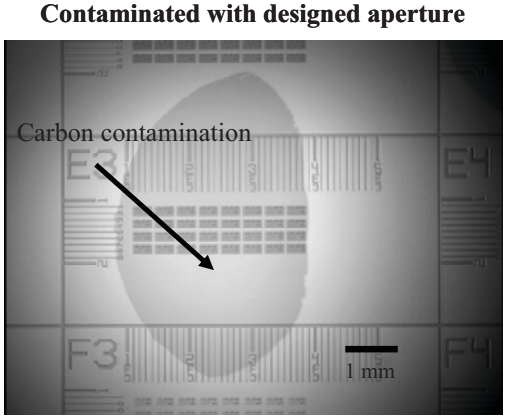

Fig. 2. A 3 by 5 mm aperture was designed to contaminate the desired EUV mask within a selected area. As shown in the optical micrograph taken by a reticle SEM, the dark oval is the carbon contamination which covers a subfield on a patterned EUV mask.

Intentional contamination on EUV masks was performed using the EUV MiMICS with a series of designed experiments. Figure 3 shows a schematic layout of the EUV mask for this work. Designed features on this mask include 16~45 nm vertical and horizontal dense lines on the wafer plane (80 ~ 225 nm on the mask plane), as well as duty cycles from 4:1 to 1:4.

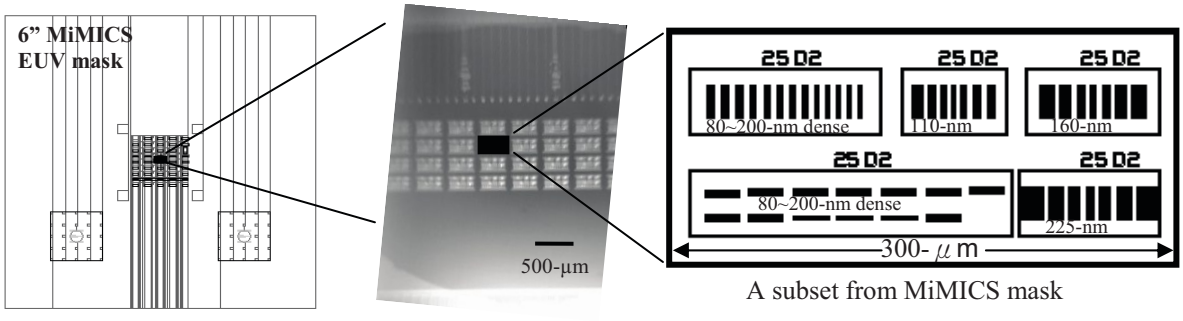

Fig. 3. A schematic view of the EUV mask layout for this work.

For this contamination work, control experiments were performed on a Si wafer. We used Filmetrix F20 [5], a broadband reflectance measurement tool, to confirm the consistency of the contamination rate. After intentional contamination, the mask was then inspected with a reticle SEM to determine the amount of carbon deposited on the mask surface. A larger CD was measured after the contamination as shown in **Figure 4**.

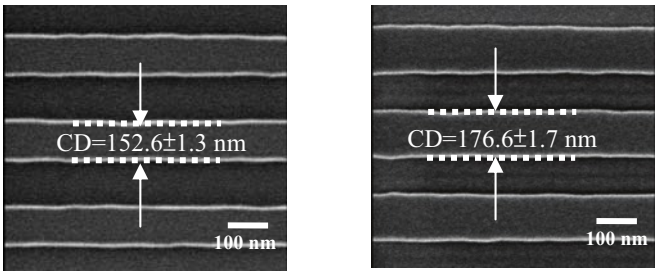

Fig. 4. Larger CD was measured after 8 hours of EUV exposure and subsequence contamination. Target CD for this measurement is 160 nm on the mask plane.

Another tool used to inspect the mask was a photoemission sensor installed on the Berkeley MET. The sensor measures a total flux of the light coming off the mask, and provides a relative reflectivity measurement for identical design of fields on the mask. The density of carbon was assumed to be 1.5 g/cm^3 based on current literature reviews (from 0.8 ~ 2.2 g/cm^3) [6-8]. The average reflectivity loss from dark field on the mask is approximately 17% for an 8- hour of EUV exposure, which is roughly equivalent to 20 nm of carbon.

3. IMAGE PRINTING AND ANALYSIS

The main objective of this study is to understand the effect of carbon contamination on a patterned EUV mask. We utilized the SEMATECH Berkeley Microfield-Exposure tool (MET) to print images on a wafer. SEM and SuMMIT software [9] were then used to analyze the imaging performance as a function of CD and dose.

Another tool used in this work is the SEMATECH Berkeley Actinic-Inspection tool (AIT), which allowed the access of aerial images on selected areas of a mask. The process window and contrast curves were studied using ThroughFocus software [10].

3.1 Features printed at the SEMATECH Berkeley MET

In this experiment, selected areas on a patterned EUV mask were exposed to EUV irradiation with carbon containing molecules present for 8 hours using the MiMICS tool. The image printing was then carried out using the SEMATECH Berkeley MET, and the exposed wafers were analyzed using a SEM and the SuMMIT software.

To study the impact of carbon contamination on imaging performance, the CD was measured at the best focus as a function of dose and exposure time, which is illustrated in **Figure 5**. The dose required to print 40 nm 1:1 targets CD on the wafer is larger for the contaminated features, as well as the shadowed case.

Based on the reflectivity measurement using a photoemission sensor, we expected to see approximately 17% of additional dose will be required to print the target CD. However, the results in this experiment showed more than 50% of additional dose is needed for both shadowed and non-shadowed cases, which is larger than the simple reflectance measurement. This indicates that the contamination topography could affect the printing performance dramatically.

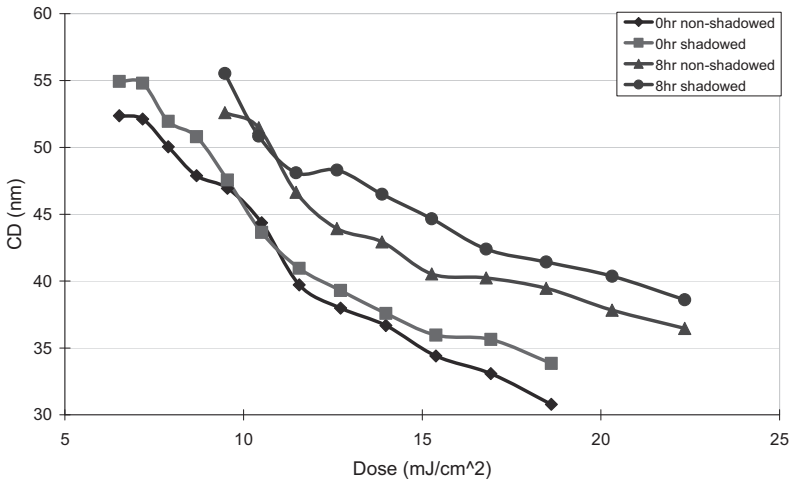

Fig. 5. For this experiment, the target CD is 40-nm. An H-V bias was observed for both contaminated and non-contaminated experiments due to the shadowing effect. Thicker carbon layer causes additional CD variation and dose shift, which results in a lower throughput.

3.2 Aerial image analysis using the SEMATECH Berkeley AIT

To understand the effect of carbon contamination on a patterned mask, the SEMATECH Berkeley actinic inspection tool (AIT) was used to record the intensity profile as aerial images from selected regions of an EUV mask.

Figure 6 shows the aerial image analysis of 200-nm 1:1 dense lines on the mask plane. Different regions of features from a clean field and two contaminated field were measured. After these images were recorded, ThroughFocus software [11] was used for aerial image data analysis and processing such as CD measurement, contrast curve, and process window. The giving dose for the process window is 9 steps, and they are 0.1, 0.2, 0.3…0.9.

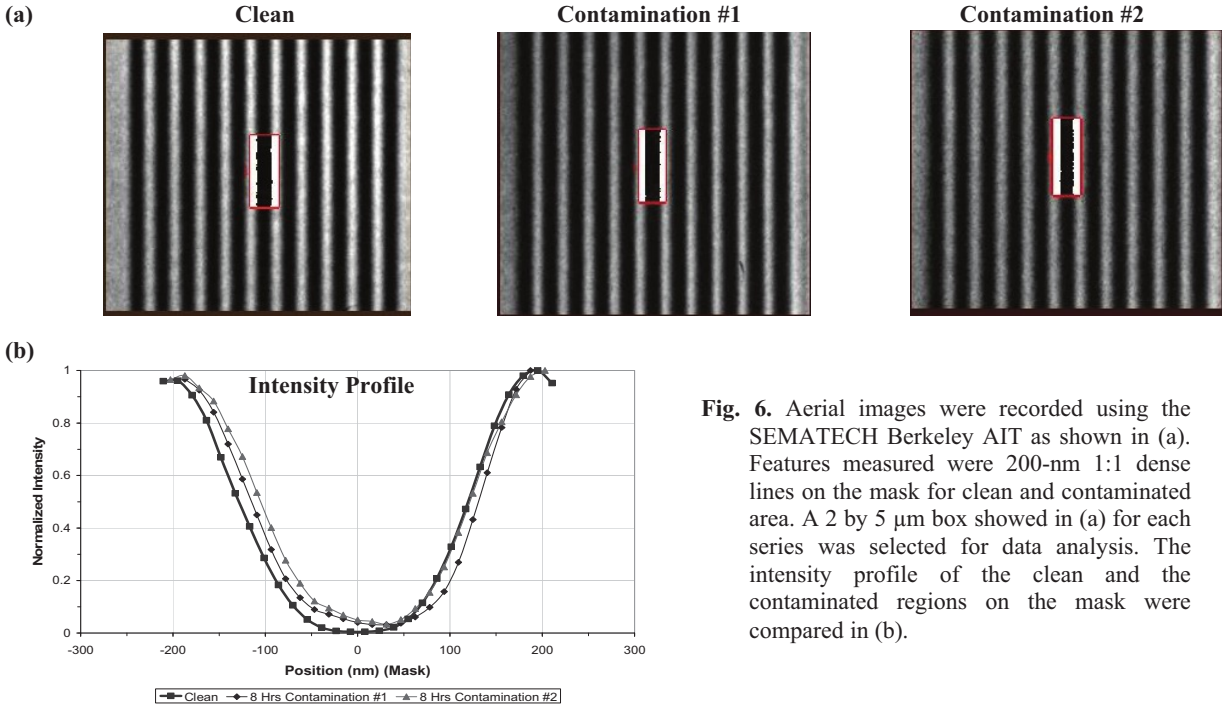

Fig. 6. Aerial images were recorded using the SEMATECH Berkeley AIT as shown in (a). Features measured were 200-nm 1:1 dense lines on the mask for clean and contaminated area. A 2 by 5 μm box showed in (a) for each series was selected for data analysis. The intensity profile of the clean and the contaminated regions on the mask were compared in (b).

Fig. 6.

(c)

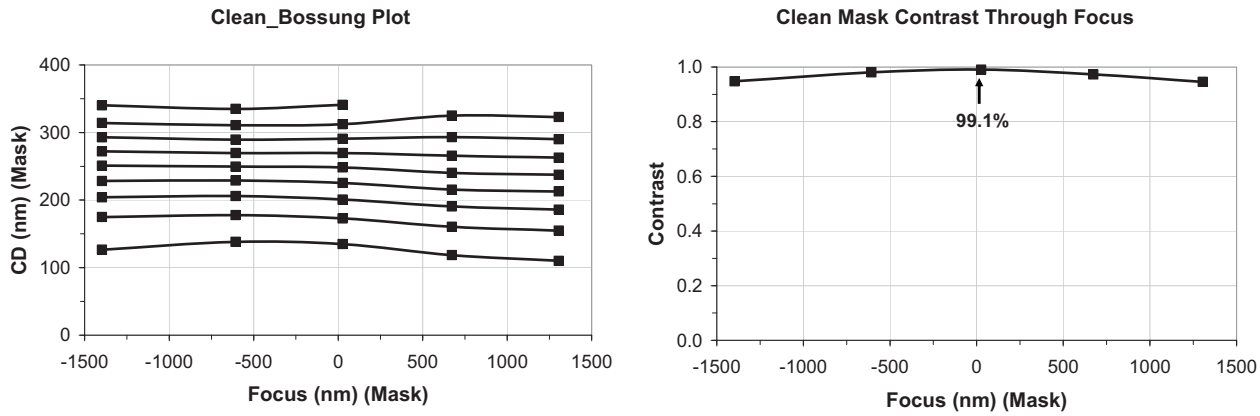

(d)

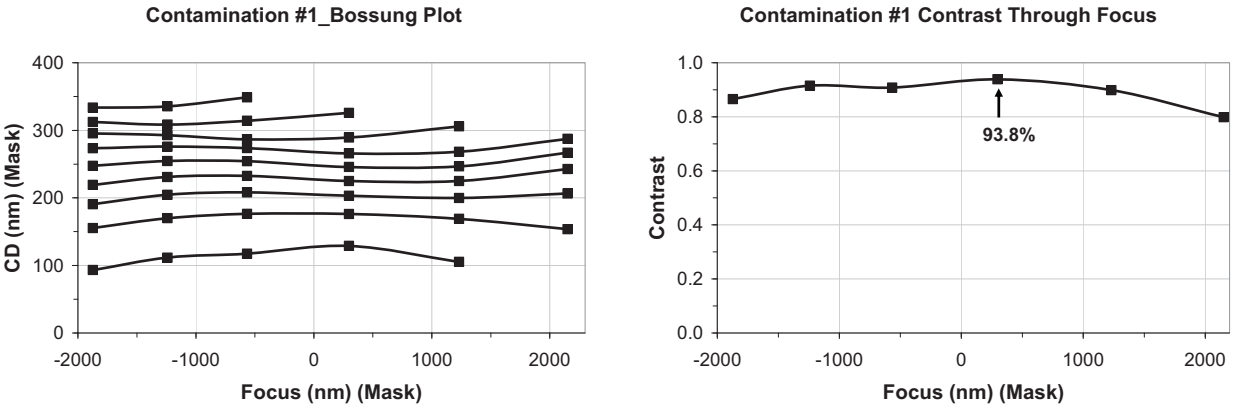

(e)

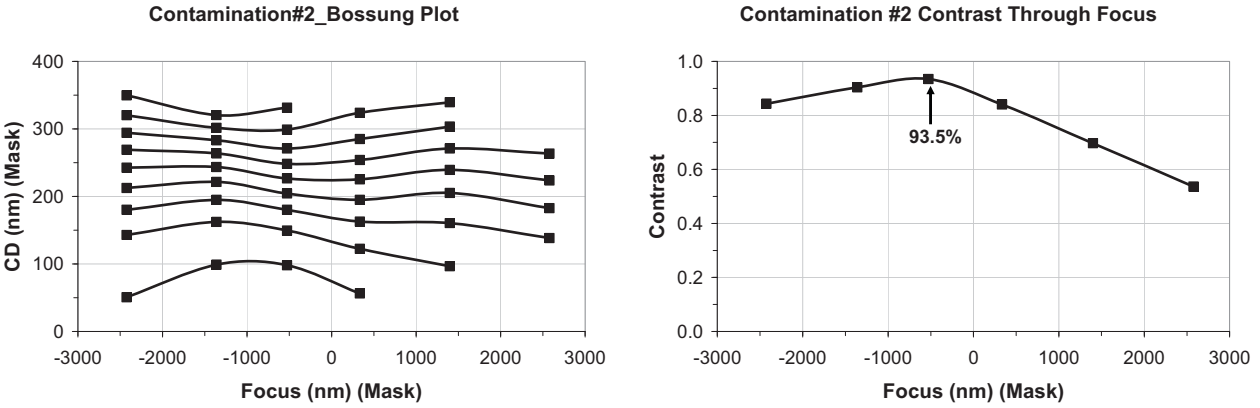

Bossung plots [11] and contrast curves were compared in (c), (d), and (e). We noticed that the peak contrast measured at the best focus showed a lower value for the contaminated features on the mask. The overall contrast and Bossung plots were worse as well, and this could affect the depth-of-focus (DOF), printing performance, and might cause a potential issue of the line width roughness (LWR).

4. SIMULATION

The impact of contamination topography of a patterned EUV mask was investigated using the EM-Suite, a lithographic software developed by Panoramic Technology Inc. which calculates the intensity reflected from a mask based on finite difference time domain (FDTD) algorithm [12].

The film stack used for both printing experiment and simulation is a Si-capped multilayer mirror, with SiO_2 as a buffer layer and TaN as an absorber layer. Feature size used for both CD measurement and simulation were 200 nm 1:1 dense lines on the mask plane. Optical parameters used for printing experiments are 0.3-NA, 4° angle-of-incidence (AOI), 5X reduction, and sigma of 0.35-0.55 annular illumination, but we used 0.25-NA, 6°-AOI, and 0.5-sigma annular illumination for the simulation. In order to reduce the complexity of this simulation, we assumed the multilayer of the mask to be defect free, and the optics aberration free as well.

4.1 Model development

Based on previous CD measurements using a reticle SEM and the Berkeley MET, we learned that the carbon thickness can be different compared to the sidewall of the absorbing features. In order to understand these effects better, we assumed two extreme cases for the possible topography, either deposited directly or conformal as shown in **Figure 7**.

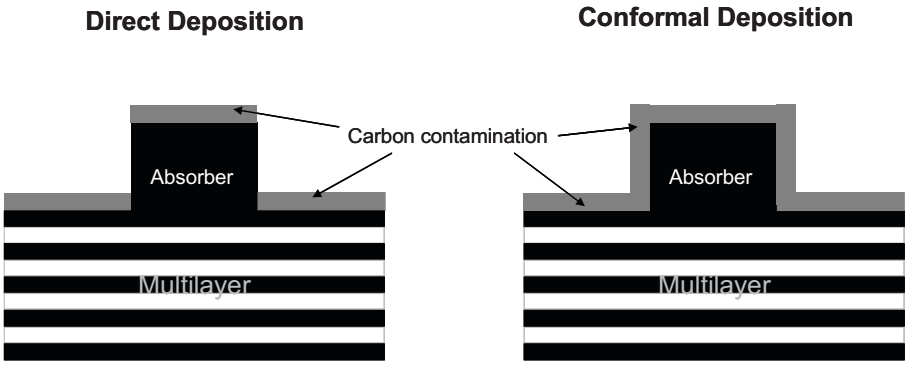

Fig. 7. Possible topography in actual exposure tool was assumed as two extreme cases, direct deposition and conformal deposition. The film stack we used is 40 bi-layers of Mo/Si with 10 nm of SiO_2 as a buffer layer, 70 nm of TaN as an absorber layer. The gray layer showed in schematic view represents the deposited carbon layer.

Both the direct and the conformal deposition cause a reflectivity drop since the undesired carbon layer absorbs the EUV radiation. In addition, the conformal deposition causes extra effects due to the growth of the carbon layer on the sidewalls, and changes the overall CD. Therefore the conformal deposition affects the imaging performance more significantly in terms of CD variation and dose shift.

4.2 Simulation results

In order to understand whether our assumptions match the experimental data, aerial images and resist parameters were calculated. As shown in **Figure 8**, the required dose to achieve the target CD vs. carbon thickness was plotted, and we observed the experimental data appears to be between the two extreme cases, direct and conformal deposition. This indicates the carbon contamination for actual topography is matched to our assumption, and could be a mix of direct and conformal deposition. Moreover, the conformal deposition requires more than 40% additional dose than the direct deposition with 30 nm of carbon layer to reach the target CD.

(a)

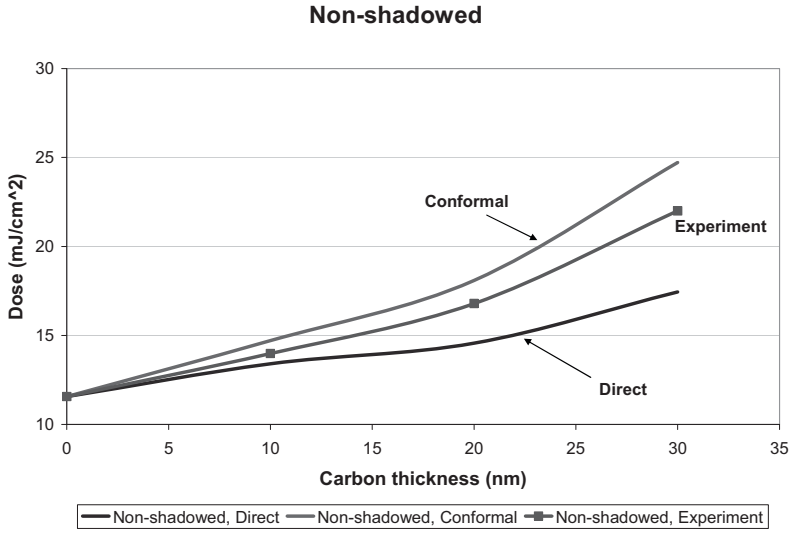

(b)

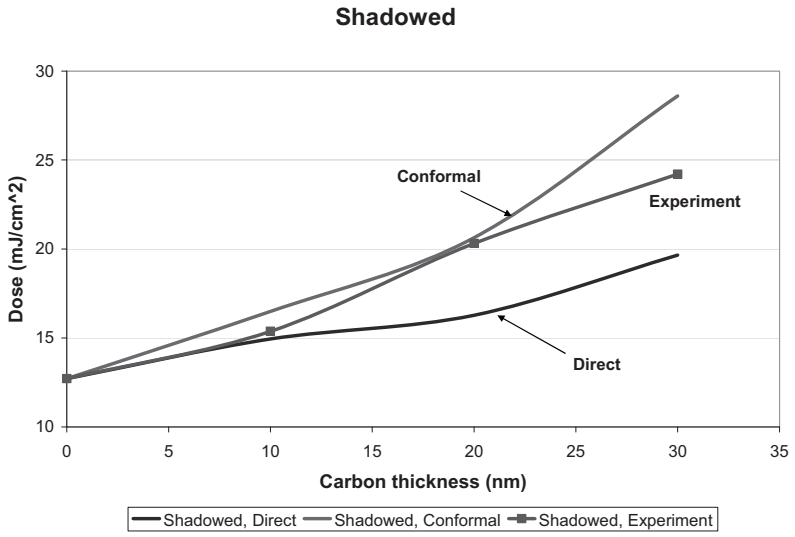

Fig. 8. In both non-shadowed (a) and shadowed (b) graphs, we observed the experimental data curves which represent the dose required to print at the target CD were between direct and conformal deposition.

We measured approximately 5 nm H-V bias between shadowed and non-shadowed features to cause the dose shift, and we applied CD compensation to correct for this factor. We then examined this compensation for a contaminated mask with carbon contamination to see if the correction is accurate.

After the CD compensation, the dose shift due to the shadowing effect was reduced. However, as shown in **Figure 9**, the two curves start to diverge when the carbon thickness is greater than 10 nm for the worst case of conformal deposition. This means the accuracy of the CD compensation could fail for 40 nm 1:1 dense lines on the wafer when more carbon is

present. In actual HVM exposure tools, smaller features, various duty cycles, or unwanted effects such as optical aberrations could make this effect more noticeable even at lower carbon thicknesses.

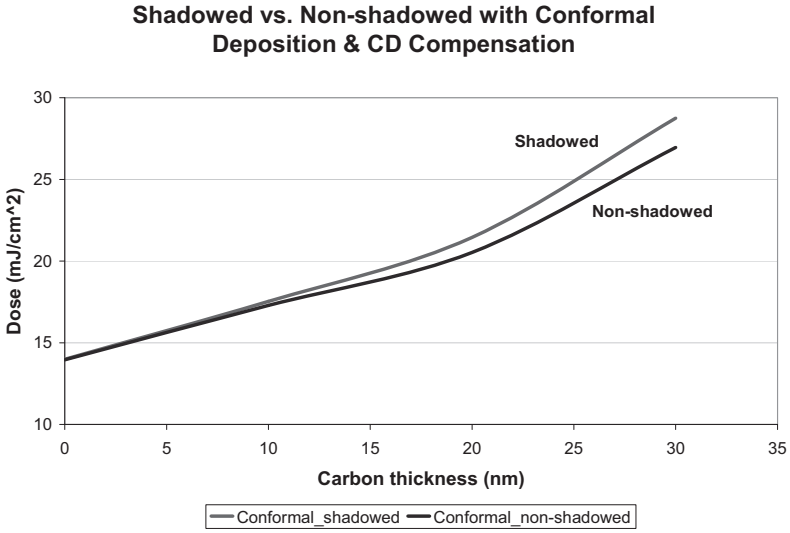

Fig. 9. Plot of the dose required to print the target CD of 40 nm 1:1 dense lines on the wafer shows a larger dose when carbon is present, as well as the divergence of the dose curves for shadowed and non-shadowed cases.

5. CONCLUSION

We used several different techniques to study the impact of carbon contamination on patterned EUV masks on imaging.

A larger mask CD after contamination was observed, increased by approximately 20 nm for an 8-hour of EUV exposure, as well as that more than 50% of additional dose was required to print the target CD. We have seen a similar effect in our simulations due to the two extreme topography assumptions, which indicates that the contamination topography could affect the printing performance significantly.

To understand the contamination topography, simulations were performed based on calculated aerial images and resist parameters. We found that the possible topography could be a mix of two extreme cases, direct and conformal deposition. The dose shift due to the shadowing effect was compensated for a clean mask in our simulation. However, this optical correction fails when the carbon thickness is greater than 10 nm for a 200 nm 1:1 dense line features on the mask. Smaller or different features, various duty cycles, or optical aberrations could make this effect more noticeable even at lower carbon thickness.

Aerial images analysis also showed a change in the through-focus contrast behavior, with the peak contrast at the best focus being reduced from 99% to approximately 93%. Accompanying effects of smaller DOF and potential LWR due to the contamination topography may be an issue.

REFERENCES

[1] P. Naulleau et al., "Status of EUV micro-exposure capabilities at the ALS using the 0.3-NA MET optic," *Proc. SPIE* 5374, *pp. 881–891*, (2004).

[2] K. A. Goldberg et al., "EUV-mask reflectivity measurements with micron-scale spatial resolution," *Proc. SPIE 6921, 69213U*, (2008).

[3] G. Denbeaux, Y. J. Fan, et al., "Accelerated contamination testing of EUV masks." *Proc. SPIE 6921-71*, (2008).

[4] http://www.panoramictech.com/

[5] http://www.filmetrics.com/

[6] J. Hollenshead and L. Klebanoff, "Modeling radiation-induced carbon contamination of extreme ultraviolet optics." *J. Vac. Sci. Technol*, *B 24(1)*, (2006).

[7] J. Hollenshead et al., *J. Vac. Sci. Technol., B 24, 64*, (2006).

[8] Y. Nishiyama et al., *Proc. SPIE, 6921, 692116*, (2008).

[9] http://www.euvl.com/summit/

[10] http://ThroughFocus.com

[11] J.W.Bossung, "Projection Printing Characterization.", *Proc.SPIE Developments in Semiconductor Microlithography II*, *vol. 100, pp. 80-84*, (1977).

[12] T. Pistor, "Expanding the Simulation Capability of TEMPEST," *Electronics Research Laboratory, University of California, Berkeley*, (1997).